Mesoscopic phenomena in Bose-Einstein systems: Persistent currents, population oscillations, and quantal phases

Yuli Lyanda-Geller and Paul M. Goldbart
Department of Physics and Materials Research Laboratory, University of Illinois at Urbana-Champaign, Urbana, Illinois 61801
(Received 9 December 1998; revised manuscript received 7 September 1999; published 17 March 2000)

Mesoscopic phenomena—including population oscillations and persistent currents driven by quantal phases—are explored theoretically in the context of multiply connected Bose-Einstein systems composed of trapped alkali-metal gas atoms. These atomic phenomena are bosonic analogs of electronic persistent currents in normal metals and Little-Parks oscillations in superconductors. Differences between oscillatory phenomena due to quantal phases in Bose-Einstein systems and in conventional superconductors are discussed, particularly with regard to their potential for discriminating between the standard BCS scenario and the Bose-Einstein condensation of preformed pairs scenario for the superconducting transition in high-temperature superconductors.

PACS number(s): 03.75.Fi, 03.65.Bz, 73.23.Ra, 74.25.Bt

I. INTRODUCTION

The purpose of this paper is to consider multiply connected many-particle systems obeying Bose-Einstein statistics and, in particular, to address the sensitivity of such systems to quantal phases [1]. Such considerations are of relevance to two areas that are currently attracting attention: Bose-Einstein condensates in atomic gases and Bose-Einstein condensation (BEC) as a scenario for the superconducting transition in high-temperature superconductors.

Multiply connected bosonic systems are now experimentally achievable in the setting of alkali-metal gas atoms confined by torus-shaped magnetic or optical traps (Fig. 1). In multiply connected systems of charged fermions wave functions can acquire Aharonov-Bohm (AB) phases, which are electromagnetic in origin. In contrast, if the bosonic constituents (e.g., alkali-metal gas atoms) are electrically neutral then electromagnetism, in the form of the AB phase, cannot provide a source of quantal phase. So, in seeking sensitivity to quantal phases we are led to consider the spin degree of freedom of the bosons, and the consequent possibility of quantal phases of geometric origin [2]. As we shall see, geometric quantal phases can readily affect the energy levels, and hence populations, of the single-particle quantum states, and lead to persistent equilibrium currents in multiply connected systems, thus providing a striking example of quantal mesoscopic phenomena in the setting of bosonic systems. Such phenomena are bosonic analogs of phenomena well known in the context of the mesoscopic physics of normal-state electronic systems (such as persistent equilibrium currents and conductance oscillations in conducting rings) which arise due to AB [3] or geometric [4–6] quantal phases. They are also bosonic analogs of the flux sensitivity of the superconducting transition temperature in thin-walled superconducting rings, known as Little-Parks oscillations [7]. (These quantum interference phenomena are mesoscopic in the sense that they vanish in the limit of large system size.)

Flux-driven phenomena in BEC systems, although similar to flux-driven phenomena in conventional superconductors, are not related to the flux-induced destruction of Cooper pairs, and arise even when interactions between bosonic species are very small. This distinction is especially important in the light of several proposals that the Bose condensation of preformed pairs of charge carriers plays a central role in the mechanism of high-temperature superconductivity (HTSC) [8–10]. The relevance of these proposals can be tested experimentally, as we shall discuss, by searching for sensitivity to magnetic flux in HTSC materials.

It is worth mentioning that there is a sense in which bosonic settings are preferable to electronic settings, if one wishes to observe implications of quantal phases in many-particle physics: in the fermionic case, the Pauli exclusion principle forces the occupation of many single-particle states, and there are strong cancellations between the effects of quantal phases on these states. By contrast, Bose-Einstein statistics promote the significance of the single-particle ground state. In this sense then, bosonic systems tend to amplify mesoscopic effects, at least in comparison with fermionic systems.

For atomic BEC systems the important question is how to introduce a nonelectromagnetic quantal phase (and the associated flux). One scheme for introducing a geometric quantal phase is to have the bosons move through regions of space in which there is a spatially varying magnetic field to which the spins of the bosons are Zeeman coupled. Then, as discussed in Ref. [11] in the context of magnetic traps, the inhomogeneous magnetic field (if sufficiently strong) leads to a geometric vector potential $\mathbf{A}$ (and a corresponding geometric flux Φ) which influences the orbital motion of the bosons, and does so in much the same way as the electromagnetic (AB) vector potential (and flux) influences the motion of electrically charged particles.

References [11] considered conventional (not AB-like) consequences of the geometric vector potential, that is, effects associated with nonzero values of the geometric field strength $\mathbf{\Omega} \equiv \boldsymbol{\nabla} \times \mathbf{A}$ (i.e., the vorticity). However—and this is the main point of the present paper—there are striking quantal AB-like consequences of the geometric vector potential itself (rather than the field strength), especially in multiply connected configurations, and even when $\mathbf{\Omega} = \mathbf{0}$ in the sample. These consequences include an oscillatory dependence on the geometric flux Φ of the energies of all single-particle levels and, thus, the equilibrium populations of these levels and, more generally, all equilibrium quantities. More-

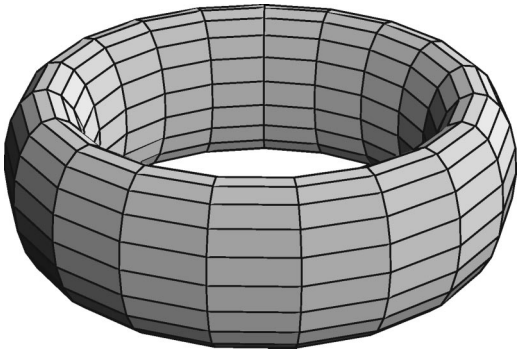

FIG. 1. Toroidal sample of noncircular cross section.

over, these single-particle energy-level oscillations lead directly to the existence of equilibrium currents [12] that flow around the trap (at generic values of Φ). Although, given the finite size of the system, there is no strict critical temperature associated with Bose-Einstein condensation, one can identify the remnant of such a critical temperature (via a crossover temperature that marks the onset of a considerable single-particle ground-state population), and this crossover temperature also oscillates with the geometric flux. Furthermore, although there is no singularity in the specific heat, there is oscillatory dependence on the temperature of the peak in the specific heat. Being *mesoscopic*, these oscillatory phenomena vanish in the thermodynamic limit. Therefore, despite the electrical neutrality of the atoms in BEC systems, the geometric phase allows one to realize counterparts of the well-established collection of electromagnetic AB-phase-sensitive phenomena, as well as new, bosonic, phenomena such as large oscillations in the populations of the various single-particle levels.

In order to realize geometric-phase-driven oscillations one needs to vary the inhomogeneous magnetic field that the bosons inhabit. In magnetic traps the ability to make such variations is limited, as variations alter the structure of the trap (i.e., the shape of the system). The recent achievement of confinement via purely optical traps [15] liberates the magnetic field from its dual role of confining the atoms *and* causing the geometric phase, and thus enlarges the scope for exploring the effects of geometric phases. In both magnetic and optical traps it is also feasible to introduce another quantal phase of nonelectromagnetic origin: the spin-orbit quantal phase. In particular, a scheme has been proposed for observing the Aharonov-Casher effect [16] in BEC systems [17], the origin of this effect being a radial electric field passing through a toroidal sample [18]. This scheme had previously been proposed in the context of superfluid ^{3}He in Ref. [19].

The present paper is organized as follows. In Sec. II we demonstrate how geometric phase (and the associated flux) arises in an inhomogeneous magnetic field in the context of multiply connected samples. In Sec. III we compute the dependence of the number of particles in a model noninteracting BEC system on the flux, and the consequences of this dependence for several physical quantities are discussed in Sec. IV. Then, in Sec. VI, we deal with the experimental issues of geometric flux effects in atomic BEC systems, and in Sec. V we discuss briefly effects of interactions. Finally, in Sec. VII we discuss possibilities for investigating flux effects in high-temperature superconductors as a probe of the BEC-mechanism scenario for superconductivity.

II. QUANTAL PHASES AND FLUXES OF NONELECTROMAGNETIC ORIGIN

In this section we discuss how quantal phase and flux effects arise in systems of electrically neutral particles of hyperfine spin S due to their interaction with an inhomogeneous magnetic field $\vec{B}(\vec{r})$. The appearance of geometric phases in inhomogeneous magnetic fields has been considered by several authors in mesoscopic settings [4–6] and for atomic alkali gases in Ref. [11]. Our aim in the present section is to illustrate the requirements on magnetic field configurations in multiply connected samples confining Bose particles such that consequences of geometric phases can be observed.

In magnetic traps an inhomogeneous magnetic field is necessarily present, with its magnitude $|\vec{B}(\vec{r})|$ behaving as a potential well. The orientation of magnetic field $\vec{B}(\vec{r})/|\vec{B}(\vec{r})|$ is also spatially inhomogeneous for magnetic traps. In contrast, in optical traps, there is no requirement to keep particles magnetically confined, and one therefore has greater freedom in choosing what magnetic fields to apply, e.g., one in which the direction varies in space but the amplitude does not.

Let us consider Bose particles of mass M and hyperfine spin S Zeeman coupled to an arbitrary inhomogeneous magnetic field. Then the single-particle Hamiltonian is given by

$$\mathcal{H}=-\frac{\hbar^2}{2M}\nabla^2-\frac{1}{2}\mu\vec{S}\cdot\vec{B}(\vec{r}), \tag{2.1}$$

where μ is the appropriate magneton. In addressing the corresponding eigenproblem it is convenient to introduce a basis of instantaneous eigenstates of the spin problem, i.e., $\{|m;\vec{B}\rangle\}_{m=-S}^{S}$, which satisfy

$$\vec{S}\cdot\vec{B}|m;\vec{B}\rangle=\hbar m|\vec{B}||m;\vec{B}\rangle. \tag{2.2}$$

Then, if we express eigenstates $|\Psi\rangle$ of $\mathcal{H}$ in terms of these instantaneous eigenkets, together with the position eigenstates $\{|r\rangle\}$, i.e.,

$$|\Psi\rangle=\sum_{m=-S}^{S}\int d^dr\Psi_m(\vec{r})|\vec{r}\rangle\otimes|m;\vec{B}(\vec{r})\rangle \tag{2.3}$$

(where d is the dimensionality of space), the eigenproblem $\mathcal{H}|\Psi\rangle=E|\Psi\rangle$ becomes

$$\frac{1}{2M}\sum_{m'=-S^S}|-i\hbar\mathbf{I}\vec{\nabla}-\vec{\mathbf{A}}|^2_{m,m'}\Psi_{m'}(\vec{r})-\frac{1}{2}m\mu|\vec{B}|\Psi_m(\vec{r})$$
$$=E\Psi_m(\vec{r}), \tag{2.4}$$

where the $(2S+1)\times(2S+1)$ matrix valued gauge potential $\vec{\mathbf{A}}$ has elements given by

$$\vec{A}_{m,m'}(\vec{r}) \equiv i\langle \vec{r};m;\vec{B}(\vec{r})|\vec{\nabla}_r|\vec{r};m';\vec{B}(\vec{r})\rangle \tag{2.5}$$

and $\mathbf{I}$ is the $(2S+1)\times(2S+1)$ identity matrix. We may take for the instantaneous eigenstates the choice $\{|m;\vec{B}\rangle\}_{m=-S}^{S}$, given by

$$|m;\vec{B}\rangle = \exp(-i\phi S_z/\hbar)\exp(-i\theta S_y/\hbar)|m;\vec{e}_z\rangle, \tag{2.6}$$

where $\{|m;\vec{e}_z\rangle \equiv \{|m\rangle\}_{m=-S}^{S}$ are eigenstates of S_z, and θ and ϕ are, respectively, the azimuthal and polar angles parametrizing $\vec{B}$.

We now address the energy eigenproblem by making an adiabatic approximation in which transitions between distinct instantaneous spin states are omitted. This approximation amounts to removing the off-diagonal terms in Eq. (2.4), which becomes

$$\frac{1}{2M}(|-i\hbar\vec{\nabla}-\vec{A}_{m,m}|^2 + V_m(\vec{r}) - \tfrac{1}{2}m\mu|\vec{B}|)\Psi_m(\vec{r}) = E\Psi_m(\vec{r}), \tag{2.7a}$$

$$V_m(\vec{r}) \equiv \sum_{m'=-S}^{S} \vec{A}_{m,m'}\cdot\vec{A}_{m',m} - \vec{A}_{m,m}\cdot\vec{A}_{m,m}. \tag{2.7b}$$

The quantity V_m is a scalar potential arising from the adiabatic approximation in addition to the more familiar gauge potential $\vec{A}_m$. Both scalar and (Berry) gauge potential arise from the spatial variation in the orientation of the inhomogeneous magnetic field through which the particles propagate. Let us pause to mention the origin of V_m: if one directly omits the off-diagonal elements of $\vec{A}$ then one does not find the contribution V_m. On the other hand, if one makes the conventional adiabatic approximation, i.e., one omits the off-diagonal elements in the eigenproblem (2.4), then V_m emerges. It should be remarked that, despite appearances, the gauge covariance of the eigenproblem is not lost by this approximation strategy, the appropriate set of gauge transformations being the spin component (m) and position $(\vec{r})$ dependent rephasing of the instantaneous eigenstates. The last term on the left hand side of Eq. (2.4) is the Zeeman energy; it acts as a potential well, and must be attractive in a magnetic trap.

Let us discuss the conditions under which it is justified to neglect the off-diagonal terms in Eq. (2.4). First, consider the terms in Eq. (2.4) that are linear in the gauge potential. In computing, say, corrections to energy eigenvalues due to these terms, diagonal terms contribute simply additively, whereas those due to off-diagonal terms are smaller, being proportional to the square of the matrix element and divided by an energy denominator associated with the Zeeman energy scale. Therefore, even though the diagonal and off-diagonal perturbations may be numerically of the same order, their perturbation of the energy eigenvalues are not. The same is true for terms in Eq. (2.4) that are quadratic in the gauge potential. Bearing this in mind, we see that provided the Zeeman energy is large, it is reasonable to neglect the off-diagonal terms in Eq. (2.4), while keeping the corresponding diagonal terms (which are numerically of the same order). This is the adiabatic approximation: it is valid provided that

$$\frac{1}{2M}|\mathbf{I}\vec{p}-\vec{A}|^2_{m,m} \gg \left(\frac{1}{2M}\right)^2 \frac{|\mathbf{I}\vec{p}-\vec{A}|^4_{m,m'}}{\mu|\vec{B}|}_{m\neq m'}. \tag{2.8}$$

We note that this condition is more stringent than the condition that there be no ''Dirac centers'' in a trap (i.e., points at which $\vec{B}$ vanishes) but is, nevertheless, readily achievable by applying stronger magnetic fields [20].

As we have just seen, in the presence of an inhomogeneous magnetic field the adiabatic approximation leads to a scalar potential in addition to a vector potential. In the following two sections we shall ignore the consequences of this scalar potential and focus on the effects of the vector potential. Our motivation for doing this is that we wish to explore analogs of the AB effect that, owing to the geometrical character of the gauge potential, are oscillatory (cf. optical interference) in nature. By contrast, variations of the scalar potential do not generically lead to oscillatory phenomena but rather to a ''smearing'' of them. What we mean by smearing is the following. Suppose that the inhomogeneous field is varied in such a way that only the vector potential is varied. Owing to its geometric character, all Feynman paths of a given winding number acquire a common phase, and that phase depends linearly on the winding number. Thus, upon the addition of one quantum of flux all equilibrium properties return to their original values. However, if the variation of the inhomogeneous field simultaneously causes the scalar potential to vary then this pure oscillatory behavior is lost because, even for a given winding number, distinct Feynman paths acquire distinct additional dynamical phases. One strategy for avoiding the complications brought by the scalar potential is to introduce and vary an independent gauge potential (e.g., by rotating the trap) while keeping the scalar potential constant. Then the original gauge potential will manifest itself through, e.g., offsets in the oscillations of various physical quantities. A second strategy involves devising a setting in which dynamical phases cancel so that interference is controlled solely by the geometric phase. (An example of this strategy can be found in Ref. [5].) In Sec. VI we shall discuss such ways to isolate the effects of the vector potential in various experimental settings.

III. MODEL MULTIPLY CONNECTED SYSTEM

In order to see some explicit thermodynamic consequences of quantal phases in multiply connected mesoscopic Bose-Einstein systems we now explore a simple model in some detail. To this end we consider a system of many identical charge-neutral noninterating bosonic atoms of mass M, confined to a multiply connected trap. For the sake of simplicity, we envisage the trap as having the following features. (i) It is toroidal and axisymmetric. (ii) It is sufficiently narrow in the radial direction that, under operating conditions, only the state with the lowest radial quantum number is occupied (i.e., the radial energy scale $\hbar\Omega_r$ is large). (iii) In the

axial direction there is confinement by an oscillator potential. (iv) If the trap is optical then only mild conditions need be obeyed if an applied inhomogeneous magnetic field is not to change the trapping potential appreciably. (v) If the trap is magnetic then the application of an additional homogeneous field will change the flux Φ but not the number of particles. In the absence of Φ, the spectrum of single-particle energy eigenvalues $\mathcal{E}^0_{q,n}$ is given by

$$\mathcal{E}^0_{q,n} = \hbar\Omega_z n + \hbar\Omega_\phi q^2, \tag{3.1}$$

where $\hbar\Omega_z$ is the axial oscillator energy scale, $\hbar\Omega_\phi$ is the azimuthal energy scale, we have omitted all zero-point energy contributions, and we do not allow for radial excitation. The quantum numbers q and n range, respectively, over all integers and all non-negative integers.

We now suppose that the toroidal system of trapped atoms is subjected to a magnetic field having the property that the orientation of the field varies across the trap. Under conditions of adiabaticity for the dynamics of the spins of the atoms discussed in Sec. II, the dominant effect of the inhomogeneous magnetic field on the energy spectrum is to introduce a spin-dependent flux Φ [21], so that the spectrum (for atoms with spin projection lying parallel to the magnetic field) becomes

$$\mathcal{E}_{q,n} = \hbar\Omega_z n + \hbar\Omega_\phi (q-\Phi)^2. \tag{3.2}$$

(Atoms with spin projection lying antiparallel to the magnetic field direction are not trapped.) The relationship between the vector potential and the resulting flux will be discussed below in Sec. VI. As we shall see there, the value of the flux is determined by the area on the unit sphere of the magnetic field orientations that is subtended by orientations of the field encountered by spins of particles that follow semiclassical trajectories in a trap.

Our aim is to compute the number of particles in the single-particle ground state as a function of the temperature T, the geometric flux Φ, and the mean total number of particles N, and to do so via the grand canonical ensemble [22]. To this end, we first compute the total number of particles N as a function of T, Φ, and the chemical potential μ:

$$N(T,\Phi,\mu) = \sum_{q=-\infty}^{\infty} \sum_{n=0}^{\infty} N_{q,n}, \tag{3.3a}$$

$$N_{q,n} \equiv \{e^{(\mathcal{E}_{q,n}-\mu)/k_B T} - 1\}^{-1}. \tag{3.3b}$$

Next, we decompose this sum: $N = \tilde{N} + \hat{N}$, where

$$\tilde{N} \equiv \sum_{q=-\infty}^{\infty} N_{q,0}, \quad \hat{N} \equiv \sum_{q=-\infty}^{\infty} \sum_{n=1}^{\infty} N_{q,n}. \tag{3.4}$$

To compute $\tilde{N}$, we use a variant of the contour integration technique described, e.g., in Refs. [23], which yields

$$\tilde{N} = \frac{\pi}{2\varphi}\{\cot\pi(\Phi-\varphi) - \cot\pi(\Phi+\varphi)\} + O(\exp[-(2\pi)^{3/2}/\tilde{\Omega}_\phi^{1/2}]), \tag{3.5}$$

where we have introduced the reduced frequency $\tilde{\Omega}_\phi \equiv \hbar\Omega_\phi/k_B T$ and the reduced chemical potential $\tilde{\mu} \equiv \mu/k_B T$ and, for convenience, φ denotes $(\tilde{\mu}/\tilde{\Omega}_\phi)^{1/2}$. [The form for $\tilde{N}$ arrived at by this technique is much more rapidly convergent than the original form, Eq. (3.3a).] Not surprisingly, however, even after omitting exponentially small terms, the transcendental equation for $\tilde{\mu}(T,\Phi,\tilde{N})$, Eq. (3.5), cannot, in general, be solved explicitly. Without loss of generality, let us assume that $0 \leqslant \Phi \leqslant 1/2$. (Results for other values of Φ can be obtained via the symmetries of reflection, $\Phi \to -\Phi$, and translation, $\Phi \to \Phi + 1$.) Then further simplification is achievable in three cases: (i) $\Phi \ll 1/2$, (ii) $\Phi \gg (\tilde{N}\tilde{\Omega}_\phi)^{-1/2}$, and (iii) $|\cot 2\pi\Phi| \gg \tilde{N}\tilde{\Omega}_\phi\Phi/\pi$. In case (i) we expand the cotangents on the right hand side of Eq. (3.5) in Laurent series, retaining two terms in each series, and solve the resulting equation for $\tilde{\mu}$, thus arriving at

$$\tilde{\mu} \approx \tilde{\Omega}_\phi\Phi^2 - \{\tilde{N} - (\pi/3\tilde{\Omega}_\phi)\}^{-1}. \tag{3.6}$$

In case (ii) we instead expand the prefactor and the arguments of the cotangents in Eq. (3.5) to linear order in the deviation of $\tilde{\mu}$ from the (dimensionless) single-particle ground-state energy $\tilde{\Omega}_\phi\Phi^2$. Thus, we arrive at

$$\tilde{\mu} \approx \tilde{\Omega}_\phi\Phi^2 - 2\pi^{-1}\Phi\cot^{-1}(\cot 2\pi\Phi + \pi^{-1}\Phi\tilde{\Omega}_\phi\tilde{N} + \sqrt{\cot^2\pi\Phi + (\Phi\tilde{\Omega}_\phi\tilde{N}/\pi)^2 + 1}). \tag{3.7}$$

In case (iii), which corresponds to Φ close to 1/2, we have

$$\tilde{\mu} \approx \tilde{\Omega}_\phi\Phi^2 - 2\pi^{-1}\Phi\cot^{-1}(\Phi\tilde{\Omega}_\phi\tilde{N}/\pi). \tag{3.8}$$

In making our expansions of Eq. (3.5) for $\tilde{N}$ we restrict ourselves to the regime of quasi-BEC, i.e., we consider values of μ only slightly smaller than the single-particle ground-state energy $\mathcal{E}_{0,0}$ (i.e., $\hbar\Omega_\phi\Phi^2$).

IV. PHYSICAL CONSEQUENCES OF THE GEOMETRIC FLUX

To use these results for $\tilde{\mu}(T,\Phi,\tilde{N})$ to determine desired physical quantities, such as the populations $N_{q,n}$ of the single-particle states as functions of the variables (T,Φ,N), we first note that in the regime of BEC we need only retain the difference between μ and $\mathcal{E}_{0,0}$ in $\tilde{N}$, but may omit it from $\hat{N}$ (i.e., in the formula for $\hat{N}$ we may replace μ by $\mathcal{E}_{0,0}$). Next, we observe that $N \equiv \tilde{N} + \hat{N}$, so that by knowing $\tilde{\mu}(T,\Phi,\tilde{N})$ we know $\tilde{\mu}(T,\Phi,N)$. This we use to eliminate μ from the Bose functions that determine the populations $N_{q,n}$, which, as desired, we thus know as functions of (T,Φ,N). For example, to obtain the analytical result for the ground-state population $N_{0,0}$ at $|\Phi| \ll 1/2$ we use Eq. (3.6) to

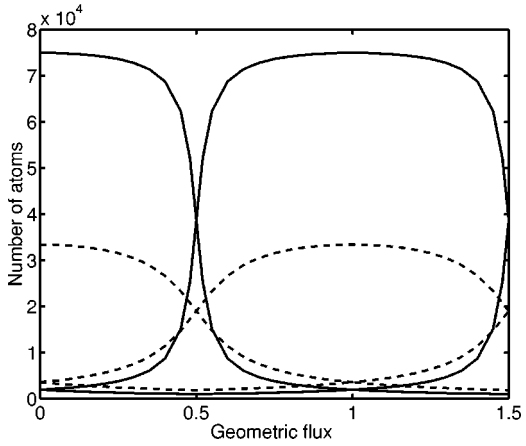

FIG. 2. Oscillatory dependence on the geometric flux of the populations of the lowest three single-particle energy levels at a higher (dashed line) and a lower (full line) temperature. At $\Phi=0$ the state characterized by $q=0$ has the biggest population for each temperature.

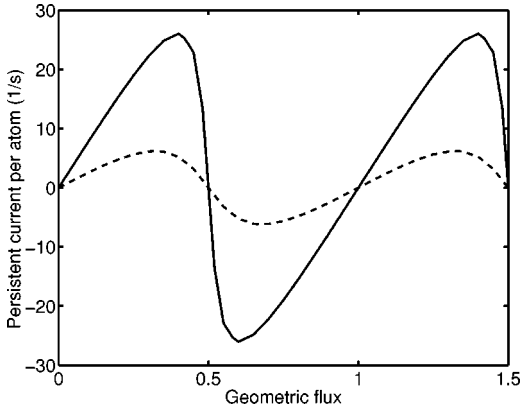

FIG. 3. Oscillatory dependence of the equilibrium persistent particle current (per atom) on the geometric flux at a higher (dashed line) and a lower (full line) temperature.

eliminate $\tilde{\mu}$ from Eq. (3.3b). To illustrate the oscillatory behavior of single-particle state populations with Φ we show, in Fig. 2, the populations $N_{q,m}$ of the three lowest-lying states (i.e., $N_{0,0}$, $N_{1,0}$, and $N_{2,0}$, as $|\Phi|\leqslant 1/2$) as functions of Φ [24]. We have chosen for this illustration a system of $N=10^5$ atoms of ^{87}Rb, sample radius $R=1$ μm, axial trap frequency $\Omega_z=7500$ Hz, temperature $T=5$ μK (for which $800\tilde{\Omega}_\phi=40\tilde{\Omega}_z=1$) or $T=10$ μK (for which $400\tilde{\Omega}_\phi=20\tilde{\Omega}_z=1$), where $\tilde{\Omega}_z\equiv\hbar\Omega_z/k_BT$. The characteristic temperature of Bose condensation in these cases (the notion of the critical temperature is valid only in the thermodynamic limit) is around 50 μK. Note that at $\Phi=0$ we have $N_{q,n}=N_{-qn}$, and at $\Phi=1/2$ we have $N_{q,n}=N_{q+1,n}$. The latter case illustrates the more general point that at half-integral values of Φ the lowest single-particle energy level is degenerate for the case of perfectly azimuthally symmetric traps. If, however, the azimuthal symmetry is absent then the level crossing is avoided, and the single-particle ground state is separated from the excited states by an energy gap at all values of Φ.

The population oscillations are mesoscopic, in the sense that they vanish in the thermodynamic limit [25]. Indeed, the number of atoms in traps, although typically large, is not on the order of Avogadro's number and, therefore, the systems are even further from the thermodynamic limit than conventional macroscopic and even mesoscopic samples. Nevertheless, although BEC is not, strictly speaking, marked by a sharp thermodynamic phase transition, atomic condensates already acquire features of the thermodynamic limit at $N=10^4$ (see, e.g., Refs. [26,27]). Despite this, our calculations reveal oscillatory phenomena at $N=10^5$ whenever the fraction of atoms in the ground state is appreciable. Thus, one has the capability of observing, simultaneously, both macroscopic and mesoscopic phenomena.

The Φ dependence of the single-particle energy levels also leads to the phenomenon of equilibrium persistent currents, i.e., dissipationless particle currents that flow around the trap. (Such equilibrium currents should, of course, be distinguished from the nonequilibrium metastable currents that can arise in multiply connected samples; see, e.g., Refs. [12].) The simple formula

$$I=\sum_{q=-\infty}^{\infty}\sum_{n=0}^{\infty}N_{q,n}\partial\mathcal{E}_{q,n}/\partial\Phi \tag{4.1}$$

for the persistent particle current I follows from the general relation $\delta F/\delta\mathbf{A}=-\mathbf{j}$, where F is the free energy, $\mathbf{A}$ is a gauge potential (such as the geometric vector potential), and $\mathbf{j}$ is the conjugate current density. In Fig. 3 we show the dependence of I/N on Φ at the conditions and temperatures specified in the previous paragraph. As T is increased from zero the sawtooth form of the Φ dependence is smoothed to a more sinusoidal form, but the zeros at integral and half-integral values of the flux are preserved. As for the characteristic scale of the amplitude of I, it is on the order of $N\Omega_\phi$, at least when the ground state contains most of the particles.

As it is Fermi rather than Bose systems that have traditionally provided settings for mesoscopic physics, we pause to compare the characteristic magnitudes of persistent currents in Fermi and Bose systems. In the special case of single-channel systems the characteristic magnitudes are similar: the many bosons in the (low-velocity) ground state contributing roughly as much as the single (high-velocity) fermion at the Fermi level (contributions from fermions below the Fermi level essentially canceling one another). In the more general case, however, in which there are many channels, the greater the extent of transverse excitation, the smaller the contribution to the persistent fermion current (owing to the reduced kinetic energy at the Fermi level). By contrast, for bosons the particle occupations are, of course, not spread over the many current-reduced channels, and instead are concentrated on the optimal channel. Thus, for bosonic systems such mesoscopic effects are amplified, relative to the Fermi case.

As a third consequence of the geometric flux, we consider the oscillatory behavior of the (dimensionless) specific heat (per particle) $C\equiv\partial E(T,\Phi,N)/\partial Nk_BT$. (We recognize that C may be difficult to measure.) For C, a more pronounced Φ

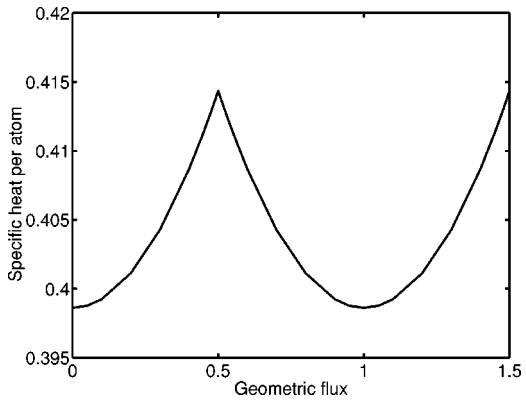

FIG. 4. Oscillatory dependence of the specific heat per atom on the geometric flux.

dependence arises in the case of traps that are weakly confining in the axial direction (i.e., $\Omega_z \ll \Omega_\phi$). In Fig. 4 we show $C(\Phi)$ for the case of ^{23}Na (the reduced mass of which also enhances the sensitivity to Φ compared with ^{87}Rb) at $R=0.5\ \mu$m, $T=40$ nK, and $\Omega_z=100$ Hz. Upon closer inspection, the apparent cusp at the level crossing, which is a remnant of the true singularity at $T=0$, is seen to be rounded.

V. ROLE OF INTERPARTICLE INTERACTIONS

The collection of many-body eigenstates of the full many-boson system is, of course, periodic in the flux Φ, regardless of the interaction strength. Thus, at least qualitatively, interactions are not expected to alter the oscillatory effects that we have discussed. In the presence of a vector-potential of nonelectromagnetic origin, the Gross-Pitaevskii equation [28] for the wave function for a neutral condensate $\psi_m(\vec{r})$ in the instantaneous spin eigenbasis reads

$$\left(\frac{\hbar^2}{2M}|-i\vec{\nabla}-\vec{A}_m|^2+U(\vec{r})+g|\psi_m(\vec{r})|^2\right)\psi_m(\vec{r})=\mu\ \psi_m(\vec{r}), \tag{5.1}$$

where the potential profile $U(\vec{r})$ is determined by the external potential, which can include potentials responsible for the magnetic and/or optical confinement of atoms and the effective scalar potential $V_m(\vec{r})$. The coupling constant g in Eq. (5.1) is related to the scattering length a, which characterizes boson-boson interactions via $g=4\pi\hbar^2 a/M$. Note that Eq. (5.1) holds in situations in which condensation occurs only in a single instantaneous spin state. Otherwise, the nonlinear term would couple the condensate wave functions for various values of m. Now, if the interboson interactions are sufficiently strong, the BEC transition has a mean-field character similar to the superconducting transition described by the Ginzburg-Landau equation, and therefore oscillatory phenomena in BEC systems would be similar to those in Ginzburg-Landau superconductors. However, atomic BECs are dilute systems, i.e., the mean number of particles in a scattering volume $\bar{n}a^3$ (where $\bar{n}$ is the average density) is much smaller than unity, which makes it feasible that the effects of the interactions are weak. However, whether or not interaction effects are indeed weak depends on the ratio of the characteristic interaction energy $E_{\rm int}\equiv gN\bar{n}$, where N is the number of particles in the condensate, and the kinetic energy $E_{\rm kin}$. It turns out that the ratio $E_{\rm int}/E_{\rm kin}$ in torus-shaped samples can be very small. Indeed,

$$E_{\rm int}\sim N\left(\frac{\hbar^2 a}{M}\right)\left(\frac{N}{Ra_1a_2}\right), \tag{5.2}$$

where R is the radius of (the centerline of) the torus, a_1 is the oscillator confinement length in the axial direction, and a_2 is the oscillator confinement length in the radial direction. As for the kinetic energy, it can be estimated as the zero-point motion energy.

The situation of interest for us is that described in Secs. III and IV, for which $R\gg a_1\gg a_2$. In this case, the kinetic energy is the energy associated with the the largest of the three zero-point energies (i.e., the radial one), so that

$$E_{\rm kin}\sim N\hbar^2/Ma_2^2. \tag{5.3}$$

Therefore, in our torus, with its highly noncircular cross section, we have

$$\frac{E_{\rm int}}{E_{\rm kin}}\sim N\frac{aa_2}{Ra_1}. \tag{5.4}$$

For ^{87}Rb, for which the scattering length a is 5.77 nm, and for a toroidal trap having the parameters discussed in Sec. IV, the ratio $E_{\rm int}/E_{\rm kin}$ can be as small as ~ 0.1. Thus, the anisotropy of the traps we are considering provides a geometric parameter that enables the effects of the interactions to be rendered small. Such interactions, nevertheless, are sufficient to allow equilibration (and therefore Bose condensation). In the present context of oscillatory phenomena, the effect of interactions on the chemical potential can thus be made rather small (i.e., $k_{\rm B}T\gg\mu$), and one therefore expects interactions to have only perturbative consequences [27].

VI. EXPERIMENTAL ISSUES OF GEOMETRIC FLUX EFFECTS IN ATOMIC CONDENSATES

A. Basic issues

Having described several consequences of the geometric flux, we now discuss some issues concerning the possibility of the experimental realization of these consequences. We see three pivotal matters: (i) how to construct a toroidal sample; (ii) how to detect population oscillations and persistent currents; and (iii) how to subject the sample to a suitably inhomogeneous field. As for (i), it should be feasible to construct toroidal samples based on magnetic traps by using a blue-detuned laser to repel atoms from the trap center. We hope that in purely optical traps [15] a similar method, combining red- and blue-detuned lasers, could be employed to make a toroidal sample. As for (ii), the phonon-imaging technique [29] discussed with regard to metastable currents in the last paragraph of Ref. [14] is less difficult in the present setting of equilibrium persistent currents, owing to

the far larger magnitude of the latter. The experimental configuration could be as described in Ref. [14]: a pulse of laser light generates a local rarefaction of the condensate, which then travels as two waves, one moving clockwise, the other counterclockwise. By a nondestructive imaging technique one might then observe where the two waves meet, which would give the magnitude of the persistent current. As the speed of sound has the same order of magnitude as the characteristic velocity of the persistent current, such an experiment appears feasible. As for (iii), magnetic trap technology itself is suitable for creating the necessary textured magnetic fields. (As magnetic traps are currently used as a first stage in the loading of optical traps, creating textured fields should not impose a large additional experimental burden.) We now elaborate on the issue of suitable magnetic field configurations.

B. Magnetic field configurations

1. Quadrupole trap

For the sake of illustration, consider a quadrupole magnetic trap, to which an additional static magnetic field is applied, so that the total field $\vec{B}(\vec{r})$ has the (Cartesian) form $(B'x, B'y, -2B'z+B_0)$, where B' characterizes gradients in the field. This field can be realized by using two coils in an ''anti-Helmholtz'' configuration, i.e., with currents in coils flowing in opposite directions. A Dirac center exists in such trap. However, if the trap is made multiply connected (e.g., by ''plugging the hole'' with a repulsive laser beam which creates a potential barrier) the particles do not reach this center. For this quadrupole trap, the Cartesian components of the effective spin vector potential $\vec{A}_m$ are given by

$$m\rho^{-1}\cos\theta(-\sin\phi,\cos\phi,0), \tag{6.1}$$

where $\rho^2 \equiv x^2+y^2$, $\phi \equiv \arctan(y/x)$, and $\theta \equiv \arctan(\rho B'/B_z)$. Moreover, the scalar potential V_m is given by

$$V_m(\vec{r}) = \frac{\hbar^2|m|}{4M\rho^2}\sin^2\theta(2+3\sin^2\theta). \tag{6.2}$$

As one can see from Eq. (6.1), for this field configuration the gauge potential depends on both the ρ and z coordinates.

2. Conical magnetic field in an optical trap

A second example of magnetic field configuration, which may be useful for experiments in optical traps, is the cone-shaped magnetic field for which $\vec{B}(\vec{r})$ has components

$$(-B_0(R/\rho)\sin\phi, B_0(R/\rho)\cos\phi, B_z), \tag{6.3}$$

where B_z is the static uniform magnetic field along the axis of the torus, the tangential magnetic field (described by B_0) may be created by a current-carrying on-axis wire, and R is the radius of the (centerline of the) torus. For this configuration, the geometric vector potential $\vec{A}_m$ has components

$$\rho^{-1}m\sin\theta(-\cos\phi,-\sin\phi,0), \tag{6.4}$$

and the scalar potential is

$$V_m^o(\vec{r}) = \frac{\hbar^2|m|}{2M\rho^2}\sin^2\theta. \tag{6.5}$$

3. Aharonov-Casher effect

A gauge potential, this time topological not merely geometric, can also be created by applying a radial electric field to particles in a multiply connected trap, owing to the spin-orbit interaction. This is the Aharonov-Casher setting (see Refs. [16,17,19]). In this case, the single-particle Hamiltonian has the form

$$H = \frac{\hbar^2}{2M}\left|-i\vec{\nabla}-c^{-1}\vec{E}\times\vec{G}\right|^2 - \frac{E^2G^2}{Mc^2}, \tag{6.6}$$

where $\vec{G}$ is the magnetic dipole moment of the particle. Therefore, besides the geometric vector potential, a term quadratic in the electric field is present, similar to $V_m(\vec{r})$. As we shall discuss below, the variation of the electric field leads to the variation of this term as well, and therefore to smearing effects.

C. Consequences of the vector and scalar potentials: Oscillations and smearing

Having, in the previous subection, examined various field configurations, we now turn to the consequences of the resulting vector and scalar potentials. The spin vector potential results in the geometric (i.e., Berry) phase $\oint_C \vec{A}\cdot d\vec{r}$ acquired by the wave function of a particle propagating around a loop C. The magnitude of the phase is given by the product of the hyperfine spin projection and the solid angle Ω subtended at the origin of the sphere of orientations $\vec{B}(\vec{r})/|\vec{B}(\vec{r})|$ by the inhomogeneous magnetic field as the real-space path C is traversed. The geometric flux that corresponds to this phase is given by

$$\Phi = \frac{1}{2\pi}\oint_C \vec{A}\cdot d\vec{r}. \tag{6.7}$$

In those torus-shaped samples for which all paths of the same winding number acquire approximately the same geometric phase, the tuning of the phase leads to oscillatory variations in thermodynamic quantities, as we have seen in Secs. III and IV. Any variation in the phases acquired by particles following different paths with the same winding number has the effect of smearing these oscillations (see the remarks near the end of Sec. II). Such smearing is similar to that of the oscillations in the conductivity of mesoscopic rings in a *homogeneous* magnetic field, which arises from the variation in the magnetic fluxes enclosed, e.g., by trajectories near the inner and outer edges of the ring. For BEC systems in a cone-shaped magnetic field in an optical trap, it is possible to make this smearing small by confining the condensate to a torus that is sufficiently thin in the radial direction, because for this particular field the vector potential, Eq. (6.4), is uni-

form along the axis. By contrast, in a quadrupolar trap, even if thin, the smearing would remain, owing to the nonuniformity of the vector potential along the axis [i.e., due to the z dependence of θ; see Eq. (6.1)]. The attempt to evade this smearing by opting for stronger confinement in the axial direction would, in this setting, tend to make the system more one dimensional (the only large direction being the tangential one), which tends to make Bose condensation very difficult.

As for the scalar potential $V_l(\vec{r})$, this also leads to the smearing of oscillatory effects in BEC systems, because any tuning of the geometric phase (and hence geometric flux) by the varying of the magnetic field would lead to the simultaneous variation of the effective scalar potential that does not have the requisite periodicity. This source of smearing is also predicted to manifest itself in mesoscopic physics, where it would result in the smearing of conductivity osciilations in rings containing, e.g., a magnetization texture due to domain walls [6]. Note that in BEC systems that have large hyperfine spins the smearing effects of $V_l(\vec{r})$ are less pronounced than they are in the cases of oscillatory effects for (spin 1/2) ballistic electrons, or the (spin 1) settings of diffusive electrons correlated by disorder or interactions. The reason for this is that for the larger spins arising in BEC systems, a relatively small variation in Ω would result in a full period of oscillations. [Quantitatively, $\mathbf{A}^2 \propto m^2$ whereas $V_m(\vec{r}) \propto l$.] Smearing due to $V_l(\vec{r})$ is present for any magnetic texture and, in particular, for both quadrupolar magnetic traps and cone-shaped textures in optical traps [see Eqs. (6.2),(6.5)]. One way to avoid manifestations of $V_m(\vec{r})$ in BEC systems is to investigate quantization of circulation in *rotating* traps (i.e., the Hess-Fairbank effect; see, e.g., Ref. [30]). In this case, the geometric phase would lead to a modulation of the Hess-Fairbank effect without any variation in $V_m(\vec{r})$ and therefore without any smearing.

VII. FLUX EFFECTS DUE TO PREFORMED BOSONS IN SUPERCONDUCTING MATERIALS

Flux effects in Bose-Einstein condensates, although similar to magnetic flux effects in superconductors, nevertheless differ from them in the following respects. In a superconducting state, the effect of a magnetic field is to suppress the superconductivity by destroying Cooper pairing. Such suppression occurs due to effects of the magnetic field on the orbital motion of the electrons and via the Zeeman splitting of states with the same spatial wave functions but opposite spin projections. On the other hand, the usual BEC transition is not related to pairing, and geometric (as well as electromagnetic for charged bosons) flux effects arise due to the variation of the single-particle energy spectrum, and the consequent variations in the thermal populations of the single-particle levels. In particular, as we have seen, oscillatory effects in BEC systems can arise, even when interactions between the bosons are very small.

In the context of high-temperature superconductivity, the possibility that the transition is due to the BE condensation of preformed pairs of charge carriers is currently under consideration [8–10]. These preformed pairs (which are bosonic) can have various origins, as discussed by Anderson and co-workers [31] and Emery and Kivelson [10]. If this possibility of superconductivity via the BEC of preformed bosons is indeed realized then oscillations in the level populations, equilibrium persistent currents, and perhaps specific heat, similar to those described in the present paper, may arise as consequences of an applied magnetic flux.

How can one distinguish between the BCS and preformed pairs scenarios for superconductivity on the basis of the oscillatory flux dependences of various quantities? Consider the effect of a magnetic flux threading a ring- or cylinder-shaped sample. In the BCS case, one expects Little-Parks oscillations [7] in the resistance at temperatures close to critical. Oscillations in the resistance are also expected in the preformed pairs scenario. However, the two scenarios may be distinguished by their response to the application of an additional, uniform static magnetic field, *perpendicular* to the axis of the ring or cylinder. The reason for this is that in the BCS scenario magnetic fields on the scale of the critical temperature tend to suppress pairing, and hence oscillations. By contrast, in the preformed pairs scenario the scale of fields necessary for suppression corresponds instead to the (potentially far higher) pair-formation (crossover) temperature and, therefore, fields at the scale of the superconducting critical temperature would barely suppress oscillations. We note that in order to avoid requiring unreasonably strong magnetic fields, it is necessary to consider superconductors having $T_c \lesssim 20$ K. Thus, the underdoped cuprates $YBa_2Cu_3O_y$, $La_{2-x}Sr_xCu_4$, and overdoped $Bi_2Sr_{2-x}La_xCuO_y$ provide candidates, as does the organic superconductor $(BEDT)_2Cu(NCS)_2$. [It is worth mentioning that in low magnetic fields (compared to T_c) a magnetoresistance due to Zeeman suppression of superconducting fluctuations above the transition temperature [32] arises in superconductors with the BCS scenario only close to the superconducting transition. In superconductors with preformed pairs this effect will occur in a much broader temperature range.] Furthermore, one can distinguish two scenarios of superconductivity in the Little-Parks oscillations experiment by applying the terahertz ac field instead of using the Zeeman effect in uniform magnetic field perpendicular to the axis of the ring or cylinder. We also note that Kawabata *et al.* [33] have already attempted to measure persistent currents in $YBa_2Cu_3O_y$, and report observing an oscillatory signal in the magnetic field dependence of the magnetization above T_c. However, the reported phase-breaking lengths of 40 μm seem unreasonably large. Further experiments, including that proposed in the present paragraph, could clarify the relevance of the preformed pairs scenario.

ACKNOWLEDGMENTS

We gratefully acknowledge useful discussions with A. Balaeff, C. Bender, A. J. Leggett, and the participants of the UIUC/CNRS Workshop on Bose-Einstein Condensation (November 1998). This work was supported by the Department of Energy, Division of Materials Sciences, Grant No. DEFG02-96ER45439.

[1] The present paper constitutes a substantially amplified version of Y. Liyanda-Geller and P. M. Goldbart, e-print cond-mat/9812159.
[2] M. V. Berry, Proc. R. Soc. London, Ser. A **392**, 45 (1984).
[3] A. G. Aronov and Yu. V. Sharvin, Rev. Mod. Phys. **59**, 755 (1987).
[4] See, e.g., D. Loss, P. M. Goldbart, and A. V. Balatsky, Phys. Rev. Lett. **65**, 1655 (1990); A. Stern, *ibid.* **68**, 1022 (1992); D. Loss, H. Schoeller, and P. M. Goldbart, Phys. Rev. B **48**, 15 218 (1993).
[5] A. G. Aronov and Y. Lyanda-Geller, Phys. Rev. Lett. **70**, 343 (1993).
[6] Y. Lyanada-Geller, I. L. Aleiner, and P. M. Goldbart, Phys. Rev. Lett. **81**, 3215 (1998).
[7] W. A. Little and R. D. Parks, Phys. Rev. Lett. **9**, 9 (1962).
[8] Y. J. Uemura, Physica C **282-287**, 194 (1997); V. B. Geshkenbein, L. B. Ioffe, and A. I. Larkin, Phys. Rev. B **55**, 3173 (1997).
[9] The possibility of the superconducting transition as a BEC of preformed bosons has been discussed prior to discovery of high-temperature superconductors by A. J. Leggett, J. Phys. (Paris), Colloq. **41**, 19 (1980); and P. Nozieres and S. Schmitt-Rink, J. Low Temp. Phys. **59**, 195 (1985).
[10] V. J. Emery and S. A. Kivelson, Nature (London) **374**, 434 (1995).
[11] T.-L. Ho and V. B. Shenoy, Phys. Rev. Lett. **77**, 2595 (1996); see also T.-L. Ho, e-print cond-mat/9803231.
[12] Recently, certain *nonequilibrium* properties of BEC in toroidal traps (e.g., the stability and thermal decay of metastable current-carrying states) were considered in [13,14].
[13] D. Rokhsar, e-print cond-mat/9709212.
[14] E. Mueller, P. Goldbart, and Y. Lyanda-Geller, Phys. Rev. A **57**, R1505 (1998).
[15] D. Stamper-Kurn *et al.*, Phys. Rev. Lett. **80**, 2027 (1998).
[16] Y. Aharonov and A. Casher, Phys. Rev. Lett. **53**, 319 (1984).
[17] K. G. Petrosyan and L. You, e-print cond-mat/9810059.
[18] Imposing on a BEC system both a radial electric field and a magnetic field leading to hyperfine spin interactions would result in a spin-orbit geometric phase, considered in [5].
[19] A. V. Balatsky and B. L. Altshuler, Phys. Rev. Lett. **70**, 1678 (1993).
[20] For a discussion of adiabaticity and applicability of the concept of geometric phase, including cases when **B** is close to zero, see also Y. Lyanda-Geller, Phys. Rev. Lett. **71**, 657 (1993).
[21] We will neglect the effects of the effective scalar potential $V_m(\vec{r})$, as can be done for large values of hyperfine spin projections. $V_m(\vec{r})=0$ in the case of the electromagnetic flux that results in oscillatory phenomena in superconductors with preformed pairs (Sec. VII).
[22] Although it seems more appropriate to use the canonical (i.e., fixed particle number) ensemble, it is more straightforward to use the grand canonical ensemble, as we have done. We hope that the error incurred is negligible, at least at the particle numbers on which we are focusing.
[23] A. L. Fetter and J. D. Walecka, *Quantum Theory of Many-Particle Systems* (McGraw-Hill, San Francisco, 1971), pp. 248–250; F. Olver, *Introduction to Asymptotics and Special Functions* (Academic Press, New York, 1973), Sec. 8.
[24] For this illustration we have computed the populations numerically, using Eqs. (3.3a) and (3.3b).
[25] By the thermodynamic limit we mean $N\to\infty$, Ω_ϕ and $\Omega_z \to 0$, but with $N\Omega_r\Omega_\phi^{1/2}$ tending to a constant. In this limit, we arrive at a system that, although two dimensional geometrically, does indeed exhibit a thermodynamically sharp BEC, owing to the precise form of the density of states associated with the axial oscillator.
[26] N. J. Van Druten and W. Ketterle, Phys. Rev. Lett. **79**, 549 (1997).
[27] F. Dalfovo, S. Giorgini, L. P. Pitaevskii, and S. Stringari, Rev. Mod. Phys. **71**, 463 (1999).
[28] L. P. Pitaevskii, Zh. Éksp. Teor. Fiz. **40**, 646 (1961) [Sov. Phys. JETP **13**, 451 (1961)]; E. P. Gross, Nuovo Cimento **20**, 454 (1961).
[29] M. R. Andrew *et al.*, Phys. Rev. Lett. **79**, 553 (1997).
[30] G. B. Hess and W. M. Fairbank, Phys. Rev. Lett. **19**, 216 (1967); M. Ueda and A. J. Leggett, *ibid.* **83**, 1489 (1999).
[31] P. W. Anderson *et al.*, Phys. Rev. Lett. **58**, 2790 (1987).
[32] A. G. Aronov, S. Hikami, and A. I. Larkin, Phys. Rev. Lett. **62**, 965 (1989).
[33] K. Kawkabata *et al.*, Phys. Rev. B **58**, 2458 (1998).